ONLINE MUTATION REPORT

Heterogeneity of breakpoints in non-LCR-mediated large constitutional deletions of the 17q11.2 NF1 tumour suppressor region

H Kehrer-Sawatzki, S Tinschert, D E Jenne

J Med Genet 2003;**000**:e116 (http://www.jmedgenet.com/cgi/content/full/40/10/e116)

Neurofibromatosis type 1 (NF1) is caused by mutations of the *NF1* gene at 17q11.2. The encoded protein, termed neurofibromin, contains a Ras-GTPase activating (RasGAP) domain, which accelerates the inactivation of Ras. Homozygous inactivation of neurofibromin is associated with a dysregulation of Ras mediated signalling pathways and tumorigenesis in NF1 patients.[1 2] More than 70% of the germline mutations are intragenically distributed throughout the coding region and are protein truncating.[3 4] In 5–20% of all NF1 patients, however, heterozygous microdeletions at 17q11.2 have been identified.[5–8] These patients with microdeletions often have a severe clinical phenotype characterised by facial dysmorphy, excessive numbers of neurofibromas, and mental deficits. In the majority of cases, the deletions at 17q11.2 span 1.4 mbp and are caused by recombination between highly homologous low copy repeats (LCR), which flank the *NF1* gene at distances of ~400 kb on the proximal side and 700 kb on the distal side.[9–13] The LCRs mediating intrachomosomal deletions at 17q11.2 are derived from the *WI-12393* gene and contain sequences with high homology to 19p13.[9 11 13 14] The structure of the *NF1* gene region at 17q11.2 is further complicated by other duplicated sequences, such as the pseudogene fragments of the *SMURF2* and the *KIAA0160* genes located at 17q.[9 14] These sequences may also represent templates for unequal recombinations and subsequent deletions of the intervening chromosomal regions at 17q11.2. Indeed, five patients with large deletions in 17q spanning more than 1.4 mbp have been described.[5 9 10 15–17] Up to now, breakpoints in these patients with long range deletions have not been placed precisely within the physical map of chromosome 17q11-12, which is still uncertain for a few regions.

In this study, we determined the precise boundaries of the constitutional deletion in patient BUD who was first reported by Jenne *et al*.[10] The deletion encompasses the commonly deleted 1.4 mbp interval, and additional 3.3 mbp in a distal direction. We established the complete physical map and gene content data for the entire deletion of patient BUD distal to the *WI-12393* gene, and identified the orthologues for all human genes in the mouse genome. In the genomic interval telomeric to the distal NF1 LCR, conserved gene order is observed when comparing human and mouse except for the *schlafen* (*SLFN*) gene cluster, which is partially lost in the human genome. Hence the distal break in this patient occurred in a genomic region which has experienced several local rearrangements during primate and rodent evolution.

Key points

- Deletions of the entire neurofibromatosis type 1 (NF1) region at 17q11.2 most often span the same 1.4 mbp interval and are caused by meiotic recombinations between low copy repeats (LCR) which flank the deleted interval. Several NF1 patients with even larger deletions at 17q have been reported, but the position of their breakpoints within a contiguous BAC/PAC contig has not been determined.
- The molecular characterisation of a deletion spanning more than 1.4 mbp in NF1 patient BUD is described and compared with that in four patients who have previously been characterised by marker analysis and Southern hybridisation using short genomic probes (D17S117, D17S120, D17S57, D17S73, D17S115). Both the proximal and distal breakpoints of all five patients clearly fall at different locations and are not bordered by LCRs. The centromeric break in patient BUD was mapped to BAC 271K11 at 17q11.2 between a partial SMS repeat and the WI-12393 derived LCR, whereas the distal break was located between the two SCHLAFEN (SLFN) genes, SLFN1 and SLFN3, at 17q12.
- Comparisons between the otherwise conserved human and mouse segments showed major differences in the number and orientation of SLFN genes. Thus the distal breakpoint of patient BUD lies in a region containing multiple evolutionary breakpoints. The deletion was shown to be paternally inherited and to occur through an intrachromosomal mechanism. As three of four previously analysed NF1 deletions that were not bordered by LCRs were also found to be of paternal origin, non-LCR-triggered deletions are most probably mitotic events during spermatogenesis.
- Patient BUD as well as patient UWA106-3, who also has a large deletion extending beyond the distal NF1 LCR at 17q11.2, suffer from multiple spinal neurofibromas. Their deletions may include a modifier locus which predisposes these patients to the development of these tumours.

METHODS

Patient BUD

The male 18 year old patient BUD was the first born child of dizygotic twins. Delivery was by caesarean section at 37 weeks' gestation. His birth weight was 2300 g, length 46 cm, and head circumference 32 cm. Neurofibromatosis was suspected shortly after birth, based on multiple café-au-lait spots. There was no family history of NF1.

All developmental milestones were delayed. He walked alone at five years. At age 13.8 years cognitive development was assessed at an eight year level. There were difficulties in gross and fine motor coordination.

At the age of 14, magnetic resonance imaging (MRI) of the brain showed several hyperintense T2 weighted lesions in the left and right lentiform nucleus and internal capsule on both sides. The spinal MRIs showed multiple neurofibromas affecting the nerve roots on both sides in nearly all segments of the vertebral column, often filling the neural foramina. At levels C1/2 to C4/5 and at the lumbosacral junctions, the lesions extended into the spinal canal, forming dumbbell tumours. Intraspinal tumours were present at C2/3 and C3/4. Multiple neurofibromas affecting the lumbosacral plexus were observed on both sides.

Physical examination at the age of 18 revealed 15 café-au-lait spots, skinfold freckling, and more than a thousand cutaneous neurofibromas. Height (162 cm) and head circumference (54 cm) were below the third centile. There was a thoracic scoliosis, genu valgum, deformity of the feet, and hyperextensible joints. A large fleshy nose gave his face a coarse appearance. Hands (19 cm) and feet (European shoe size 38½) were not enlarged.

FISH analysis

Chromosome spreads were prepared from lymphocytes and EBV transformed lymphoblastoid cells from the patient, and from blood lymphocytes from his father, using standard methods. BAC clones were purchased from the BACPAC Resource Center (www.chori.org/bacpac). Cloned polymerase chain reaction (PCR) products and BAC DNA used as fluorescent in situ hybridisation (FISH) probes were labelled with biotin-16-dUTP (Roche Diagnostics, Mannheim, Germany) and detected with FITC-avidin and biotinylated anti-avidin (Vector Inc, Burlingame, California, USA) or labelled with digoxygenin-11-dUTP (Roche Diagnostics) and detected by mouse anti-digoxygenin antibodies, and in a second step with anti-mouse antibody conjugated with Texas-Red (Dianova, Hamburg, Germany). Slides were counterstained with diamidinophenylindole (DAPI) and mounted with Vectashield antifade solution (Vector Inc).

PCR products used as FISH probes to narrow the deletion boundaries

PCR products were amplified from BAC DNA using the Expand Long-Template PCR system (Roche Diagnostics) and the primers listed in table 1. The PCR products were purified by GFX^{TM} DNA purification columns (Amersham Pharmacia, Freiburg, Germany) and cloned using the TOPO-TA cloning kit (Invitrogen, Karlsruhe, Germany). The authenticity of recombinant clones was confirmed by sequencing or restriction enzyme digestion. DNA was prepared from the cloned PCR products with the MIDI DNA isolation kit (Qiagen, address) and labelled by nick translation.

BAC library screening to complete the map of the 17q11.2-12 region

Filters from the RPCI-11 human BAC library and the RPC 1, 3, and 5 human PAC libraries were obtained from the German Resource Center (www.rzpd.de) and the BACPAC Resource Center (RZPD) (www.chori.org/bacpac). Screening of the libraries was done by hybridisation with markers amplified by PCR and labelled by random priming with hexamer oligonucleotides and Klenow polymerase in the presence of ^{32}P-dCTP (Amersham Pharmacia) in buffer containing 7% SDS, 0.5 M Na phosphate (pH 7.2), and 1 mM EDTA at 65°C overnight. The positions of these markers are indicated in fig 3 and the primer sequences are available from the authors by request. Filters were washed four times at increasing stringency, with a final wash of 0.2×SSC/0.1% SDS for 45 minutes. Following autoradiography for one to two days at −70°C with intensifying screens, positive clones were identified by x/y coordinates and obtained from BACPAC resources or the RZPD.

Genotyping

To determine both the parental origin of the deletion and the recombination mechanism underlying this rearrangement, marker haplotypes were reconstructed and the segregation of marker genotypes was investigated using DNA isolated from peripheral blood lymphocytes of patient BUD and his family members. Ten polymorphic microsatellite markers were analysed, five proximal (D17S841, D17S1873, D17S1841, D17S975, D17S1294) and four distal to the deletion boundaries of patient BUD (D17S907, D17S1833, D17S1788, D17S1867). Marker GGAA7D11 is located within the deleted region. Oligonucleotide primer sequences were obtained from the Genome Database and the respective forward primer was

Table 1 Cloned polymerase chain reaction products used as fluorescent in situ hybridisation (FISH) probes to confine the deletion breakpoints of patient BUD

PCR primer	Sequence (5′→3′)	BAC (GenBank accession number)	PCR product (size in bp)	Position*	FISH results
DJ2384	GGATGCAAACAGGGAGATTTT	271K11	DJ2384/2385	10862–	nd
DJ2385	GTGATGCAGG GAAGGAAAAAC	(AC005562)	(7067)	17929	
DJ2386	GGTGGCCAGTGAGGATAACAC	271K11	DJ2386/2387	30519–	nd
DJ2387	CCCAGAAGGTGACTCAGGAAG	(AC005562)	(7457)	37976	
DJ2447	GGGGGAGAACGAATGTCCAG	271K11	DJ2447/2448	40-901–	nd
DJ2448	CAGGCCTACTGCTGTGCTGTT		(8320)	49221	
DJ2516	CTGATGGCATCCTGATTTTGA	271K11	DJ2516/2517	81044–	D
DJ2517	GAACAGCAGATTCACACAAGAGC		(7230)	88274	
DJ2439	TCGTGGATTATTGCCCTTCCT	47L3	DJ2438/2439	87476–	D
DJ2438	AAGACACAGCCCCCTTCATTG	(AC022706)	(8159)	95635	
DJ2522	CTCTTATTATGGAGTGGGGAGCAG	686D22	DJ2522/2523	163300–	D
DJ2523	TCTGATCATTAGGCGAAAGACAAT	(AC060766)	(6052)	169352	
DJ2725	CATGGTACAGGATGAGGAGTTT	686D22	DJ2725/2726	26002–	nd
DJ2726	CGAAGTCTTGTAATCCAACCTG		(7300)	33302	
DJ2789	GGAAAAGCAAGATTCAAATAGTAT	686D22	DJ2789/2788	10074–	nd
DJ2788	ATTCTGGTCTTAAATACAATCTCC		(5081)	15155	
DJ2781	CTTTTCTGCCAGTCTTTCTCC	1094M14	DJ2780/2781	20271–	nd
DJ2780	CAGACCCTTATTCTCCTGCTT	(AC015911)	(6021)	26292	
DJ2730	AGTCTCTCCTTTCCCCACTTA	1094M14	DJ2729/2730	34230–	nd
DJ2729	TTACAATGGGTTGAGGAATGA	(AC015911)	(5620)	39859	

*Position of the PCR product on the respective BAC clone with respect to its accession number.
D, deleted; nd, not deleted; PCR, polymerase chain reaction.

5′ end-labelled with 6-FAM (Applied Biosystems, Foster City, California, USA). PCR products were analysed by electrophoresis on 5% denaturing polyacrylamide gels on a 396 ABI DNA sequencer using the GENESCAN (version 2.1) software (Applied Biosystems). We phased the parental haplotypes on the basis of the most parsimonious explanation of the observed genotypes.

RESULTS

Characterisation of the proximal deletion breakpoint

In a previous study, we showed by FISH analysis that BAC R-271K11 hybridised to both chromosome 17 homologues in the majority of *NF1* deletion patients, but did not produce a second signal on metaphase chromosomes of the patient BUD. The probe R-271K11s, which spans the region of BAC R-271K11 from 141950 to 148526 (according to AC005562), was clearly deleted in patient BUD, but present in the other deletion patients.[10] To locate the proximal end of the deletion in patient BUD precisely, we narrowed down the deletion boundary with additional BACs (fig 1) from the 17q11.2 region. In contrast to the more proximal BAC R-281M11, the BACs R-778K9 and 2349P21 were completely missing on one chromosome 17. We now found a highly reduced hybridisation signal with BAC R-271K11 on the second chromosome, indicating that it was not completely deleted and that some sequences from its insert still hybridised to the affected chromosome 17. Three subfragments from the proximal portion of the BAC insert were used in FISH experiments (table 1). For the PCR probes DJ2384/2385, DJ2386/2387, and DJ2447/2448, signals on both chromosomes were noted

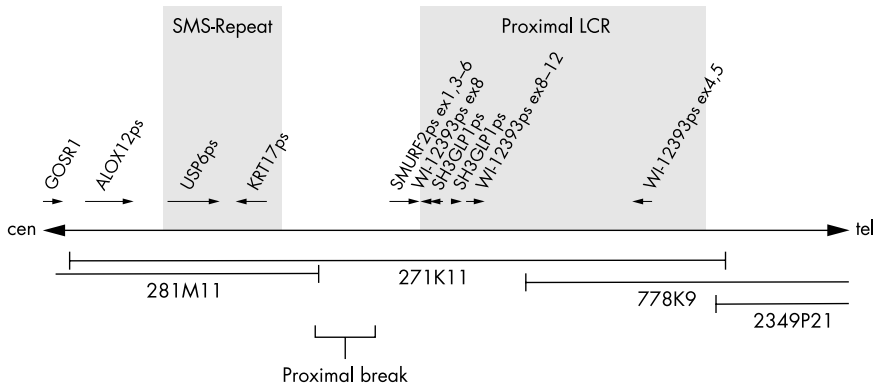

Figure 1 (A) Schematic map of the proximal deletion breakpoint region of patient BUD. The horizontal bars represent the position of BACs R-271K11 (AC005562), R-281M11 (AC011840), R-778K9 (AC023266), and 2349P21 (AC127024). Horizontal arrows indicate the transcriptional direction of the genes and pseudogenes. The low copy repeats (LCR) mapped to this region, a partial SMS (Smith-Magenis-Syndrome) repeat and the proximal *WI-12393* containing LCR, are marked by grey rectangles.

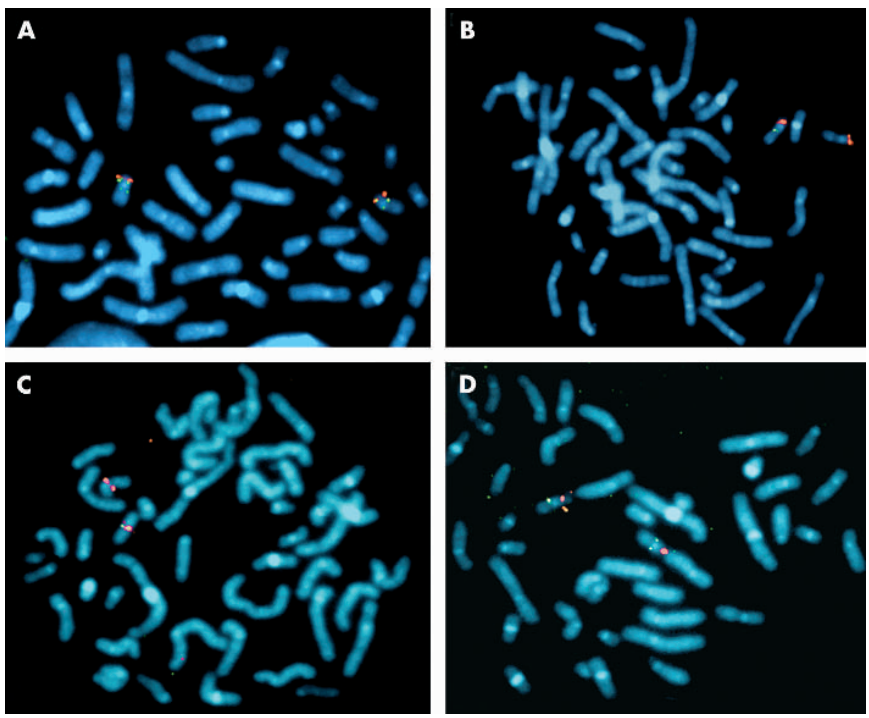

Figure 2 Confinement of the proximal (panels A and B) and distal (panels C and D) deletion breakpoints of patient BUD by fluorescent in situ hybridisation (FISH) with cloned polymerase chain reaction products (green) and, as control, BAC 1D5 (red), which maps to 17p13 (panels A, B, and D). (A) Hybridisation of probe DJ2447/2448 (green) at 17q11.2 on both homologous chromosomes. This probe also hybridised to the short arm of chromosome 17. (B) FISH analysis with probe DJ2516/2517 (green) showed a deletion of the corresponding segment of one chromosome 17. (C) FISH with probe DJ2522/2523 (green) resulted in signals only on one chromosome 17, indicating that the corresponding region is deleted. Co-hybridisation was done with BAC 1094M14 (red), hybridising to both chromosomes 17. (D) Hybridisation of probe DJ2788/2789 is detected on both chromosomes 17 and thus marks the distal deletion boundary.

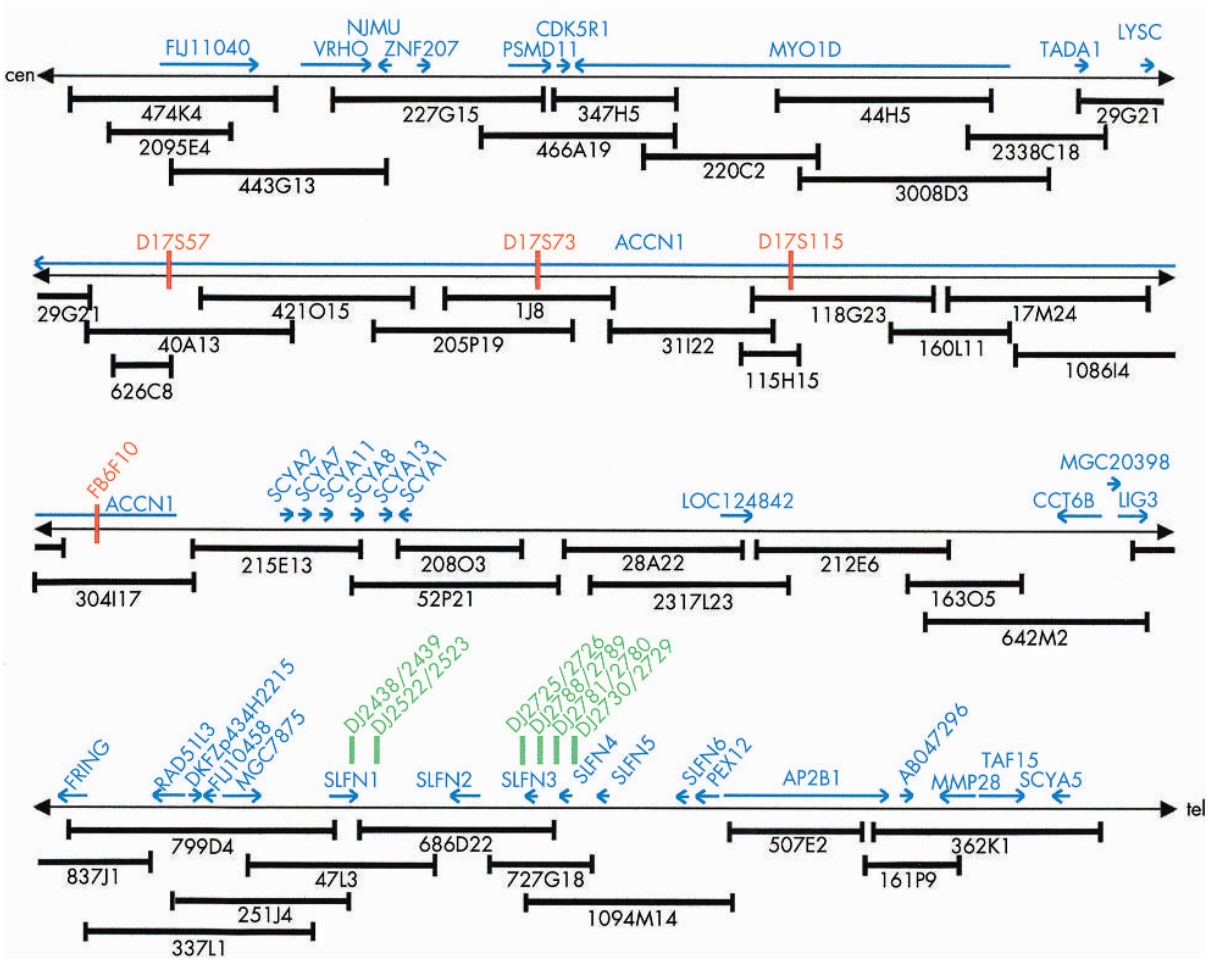

Figure 3 Schematic map of the 17q11.2-12 region from the *FLJ11040* gene, which flanks the distal LCR in the *NF1* gene region at 17q11.2 up to *SCYA5* gene. The BAC/PAC clones which make up this contig are indicated by horizontal bars. The position and orientation of the genes mapped within this region are given by horizontal arrows in blue. The location of the FISH probes (DJ2438/2439 – DJ2730/2729, in green) used to confine the distal deletion boundary of patient BUD are given, as well as those markers (red) that were previously used to investigate the deletion boundaries in other NF1 patients with large deletions.

(fig 2A), whereas probe DJ2516/2517 was clearly hybridising to only one chromosome 17 homologue (fig 2B). According to the position of the PCR primer pairs on BAC R-271K11, the proximal break occurred between 49221 and 81044 (numbering according to GenBank entry AC005562 of BAC R-271K11; table 1). Thus the proximal breakpoint of BUD lies far outside of the LCR interval (112000 and 147000 on R-271K11) which recurs on BAC R-640N20, on the distal side of the *NF1* gene.[9 11 13]

Identification of the distal breakpoint

To confine the distal end of the deletion, we assembled a BAC contig for the 3.3 mbp distal to the *WI-12393* related LCR on BACs R-640N20 and R-474K4. This contig covers the previously identified clones[18] and BAC R-337L1,[10] and ends up with BAC R-362K1, as shown in fig 3.

Overlapping clones were identified by BLAST searches using completely sequenced BAC clones, BAC end sequence, and clone pools which were screened with known STS markers from the existing radiation hybrid (Standford, Genebridge 4) and genetic linkage maps (Marshfield genetic map). This assembly was confirmed by FISH analyses with several BAC clones from this region on metaphase chromosomes from different deletion patients. The deletion of patient BUD extends up to BAC R-799D4, which is the most distal clone that is completely deleted on the affected chromosome 17. Interphase nuclei of peripheral blood leucocytes were also investigated by FISH with BAC R-799D4 and a differentially labelled BAC R-55A13 (AC015651), which maps outside of the deleted region at 17q23. The interphase nuclei of patient BUD always lacked the second signal for R-799D4 (n = 200), but displayed two signals for R-55A13. By contrast, FISH analysis with BAC R-686D22 resulted in two signals of unequal intensity on chromosome 17 homologues, indicating that this BAC is hitting the distal breakpoint region. BAC R-1094M14, which starts in the middle of R-686D22 and extends beyond its distal half, hybridised equally well to both chromosomes 17. In order to restrict the distal deletion boundary more precisely, we undertook FISH with cloned PCR products DJ2438/2439 and DJ2522/2523 (table 1; fig 3). Both probes are deleted on one chromosome 17 of patient BUD (fig 2C). Subsequently, we generated probes DJ2788/2789 (fig 2D), DJ2725/2726, DJ2781/2780, and DJ2730/2729, which hybridised to both chromosomes of patient BUD and thus delineate the distal border of the deletion. According to these observations, the distal deletion breakpoint is located in the region between the *SLFN1* and the *SLFN3* genes (fig 3).

Characterisation of the deleted interval in patient BUD and comparison with the mouse syntenic region on chromosome 11

The deletion of patient BUD encompasses 4.7 mbp including the 14 known genes between the proximal and distal *NF1* LCR at 17q11.2—*CYTOR4, FLJ12735, FLJ22729, CENT2A, MGC13061, NF1, OMG, EVI2B, EVI2A, KIAA1821, MGC11316, HCA66, KIAA0160*, and *WI-12393*—and 27 additional genes located distally to this region, ranging from *FLJ11040* to the *SCHLAFEN* (*SLFN*) gene cluster (fig 3; table 2).

Comparative analysis of the *NF1* gene region in human and mouse undertaken by us previously[14] showed that 12 of the 14 functional genes in the *NF1* gene region flanked by LCRs were also physically linked in the mouse genome on chromosome 11, but their order differed significantly.[14] The subsequent region—beginning with the *FLJ11040* gene and ending with the *SLFN* gene cluster at the distal breakpoint region of patient BUD—is, however, strictly conserved with regard to the number and arrangement of genes in both species (table 2). In the region around the distal deletion boundary of patient BUD, the human and the mouse genomes again displayed significant discrepancies. Comparing the *SLFN* genes that are bordered by the *MGC7875* and *PEX12* single copy orthologues, we noticed only six human members *(SLFN1-6)* of the *SLFN* gene family, but 10 murine genes in the otherwise conserved human–mouse interval (fig 4).

Comparison with other long range deletions of 17q

Through the last decade, three NF1 patients with large deletions at 17q11-12[5 9 15 16] and one patient with a 7 mbp deletion at 17q11.2-21[17] have been reported. The markers and FISH probes used in these studies have been identified by their sequence and placed on our physical map accordingly (fig 5). The proximal deletion boundary of patient UWA106-3

Table 2 Summary of the functional genes at 17q12 telomeric to the distal *WI-12393* derived low copy repeats (LCR) and the mouse orthologues on chromosome 11 (11B5)

Human gene (locus)	Accession No of the human cDNA	Mouse gene (locus)	Accession No of the murine orthologue	Features of the encoded protein
FLJ11040	NM_018307; AJ496730; AL136929	*Ak019059*	AK019059	ATP/GTP binding site motif A, Ca binding EF hand
VRHO	NM_138328; AJ313480	*Rhbd14*	NM_139228, AJ313479	Rhomboid-like, MT serine type peptidase, EF hand
NJMU	NM_022344; AF305686	*Ak017667*	AK017667	Highly expressed in fetal and adult testis; spermatogenesis
ZNF207	NM_003457	*Zfp207*	NM_011751; AB013357	C2H2 Zn finger, proline-rich, bipartite NLS
PSMD11	NM_002815; AB003102; AF001212	*Psmd11*	AK012951; AK007547	26S proteasome non-ATPase regulatory subunit 11
CDK5R1	NM_003885; X80343; BC020580	*Cdk5r*	NM_009871; U50707; S82819	Cyclin dependent kinase 5 activator 1; tau protein kinase II regulatory subunit
MYO1D	XM_126459; AB018270	*Myo1D*	XM_126459, BC039700	Unconventional myosin
TADA1	NM_015544; AL117619; AF132000	*Ak018332*	AK018332, BC011208	Maid-like protein
LYSC	XM_058864	*Ak006357*	AK006357	Lysozyme C
ACCN1	NM_001094; U50352; U53212	*Accn1*	NM_007384, AF348465, Y14634	ENaC related, degenerin related
SCYA2	NM_002982	*Scya2*	NM_011333	Member of SCYA family
SCYA7	NM_006273	*Scya7*	NM_013654	Member of SCYA family
SCYA11	NM_005408	*Scya11*	NM_011330	Member of SCYA family
SCAY8	NM_005623	*Scya8*	NM_021443	Member of SCYA family
SCYA13	NM_005408	*Scya12*	NM_011331	Member of SCYA family
SCYA1	NM_002981	*Scya1*	NM_011329	Member of SCYA family
LOC124842	XM_064333; BN000149; BC020591	*Loc217004*	XM_194796; BN000151	Similar to KIAA1583
CCT6B	NM_006584; D78333	*Cct6b*	NM_009839	TCP20, CCT6B, T complex protein 1, zeta 2, subunit 6B, testis specific
MGC20398	XM_039437; BC11584	*2410003C20Rik*	NM_025884	Neurofilament triplet M protein (weak) C2H2 type, NLS
LIG3	NM_002311; NM_013975	*Lig3*	NM_010716	Ligase, testis specific splice form
FRING	NM_057178	*Fring*	NM_026097	Zn finger; C3HC4 type, testis specific
RAD51L3	NM_002878; NM_133628; NM_133629	*Rad51l3*	NM_011235	DNA repair protein, RecA; ATP, GTP binding site motif A (P loop)
DKFZp434H2215	NM_017559; BC024002	*Ak019639*	AK019639	Containing FNIII domain
FLJ10458	NM_018096; AK001320	*Loc217011*	NM_145431; BC018399	G protein β; transducin-like; WD40 repeat
MGC7875 (unc-45 related)	AL832355; AL833281; XM_091530	*Loc217012*	XM_126446	Contains two armadillo repeats and a TPR domain
SLFN1	NM_144975; BC021238; AL832814; AK075116; AK054668;	*Slfn7*	AK036486	
SLFN2	NM_152270; AL512731; AK074184; AK092241; AL831964	*Slfn8*	NM_172796; XM_204663; AK036579;AK050355	
SLFN3	NM_018042; AK001122; BC035605	*Slfn9*	XM_204664;XM_137765	
SLFN4	NM_144682; AK074465; AK056514; AL833747; AL832726	*Slfn10*	XM_204665; XM_137766	
SLFN5	BN000147			
	No equivalent	*Slfn2*	NM_011408; AF099973	P loop (ATP/GTP binding site motif A)
	No equivalent	*Slfn1*	NM_011407;AF099972	P loop (ATP/GTP binding site motif A)
	No equivalent	*Slfn4*	XM_203494; XM_126110 AF099976; AF099975;	P loop (ATP/GTP binding site motif A)
	No equivalent	*Slfn3*	NM_011409, AF099974	P loop (ATP/GTP binding site motif A)
	No equivalent	*Slfn5*	XM_204667; XM_137770	
SLFN6	XM_064300	*Slfn6*	XM_137771, XM111241	
PEX12	NM_000286; U91521; AB004546	*Pex12*	BC021800; NM_134025	Peroxisome assembly protein 12

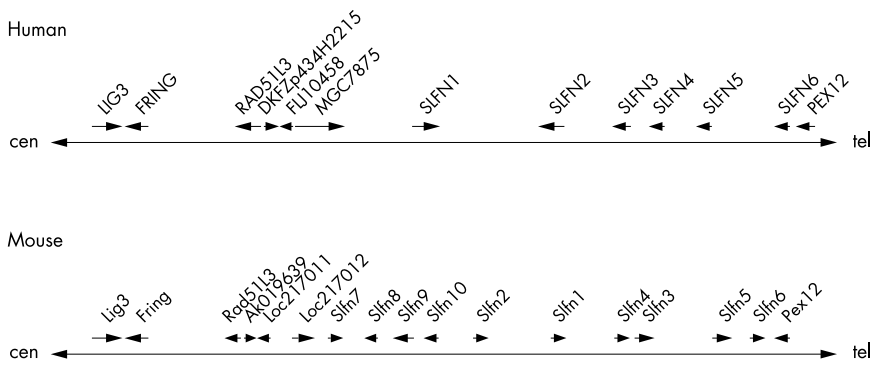

Figure 4 Comparative map of the region surrounding the distal deletion boundary of patient BUD in human and mouse. The length and the transcriptional orientation of the respective genes are indicated by arrows.

described by Kayes *et al* [15 16] was localised between D17S1294 and the *SLC6A4* gene,[19] the distal deletion breakpoint to the interval between the markers D17S73 and FB6F10 (figs 3 and 4). The proximal breakpoint of patient UWA155-1 described by Dorschner *et al* [9] was located within the LCR bordered *NF1* interval between markers SHGC35088 and FB12A2, the distal deletion breakpoint between the markers D17S1656 and stSG50857 telomeric to the LCR flanking the 1.4 mbp region.[9] The proximal breakpoint of the deletion of patient ID806[17] was located in the interval between marker D17S58 and the *CRYBA1* (Crystallin β A1) gene. Thus the proximal breaks of the five patients clearly differ in their location. The distal breakpoints of these patients, however, have not been determined precisely. In three patients—UWA106-3, UWA155-1, and patient 3724A[5]—the deletion ends in the very large *ACCN1* gene which spans more than 1 mb, including the four markers D17S57, D17S73, D17S115, and FB6F10 (figs 3 and 5). The deletion reported by Upadhyaya *et al* [17] is cytogenetically visible and is thus the largest. It ends somewhere between D17S73 and the *RARA* gene. The distal deletion breakpoint of our patient BUD is telomeric to the *ACCN1* gene in the region between the *SLFN1* and *SLFN3* genes. Blast searches with the entire *WI-12393* gene sequence did not retrieve additional LCR copies in the region between D17S58 and the *SLFN* genes.

Mechanism underlying the deletion

We analysed several polymorphic markers on 17q in the parents and two brothers of the index patient. Lack of inheritance of the paternal allele for the GGAA7D11 marker located within the deleted interval clearly indicates the paternal origin of the deletion (fig 6). Studies with markers flanking the deletion interval closely showed that the deletion arose on the paternal chromosome during spermatogenesis by an intrachromosomal mechanism.

To investigate the possibility of somatic mosaicism in BUD's father, we undertook FISH analysis with a BAC from the deletion interval, R-41C23, which flanks the *NF1* gene on the 3′ side.[10 14] On metaphase chromosomes (n = 50) and interphase nuclei (n = 50) of the father, two fluorescent signals were observed, indicating that the chromosomal deletion most probably arose during germ cell maturation.

DISCUSSION

Previous definition of the 1.4 mbp deletion interval shared by most patients with *NF1* microdeletion led to the identification and localisation of new LCRs flanking the breakpoint regions. The patient described here belongs to a small subgroup of four patients whose deletion intervals are not bordered by these LCRs. Their telomeric or centromeric

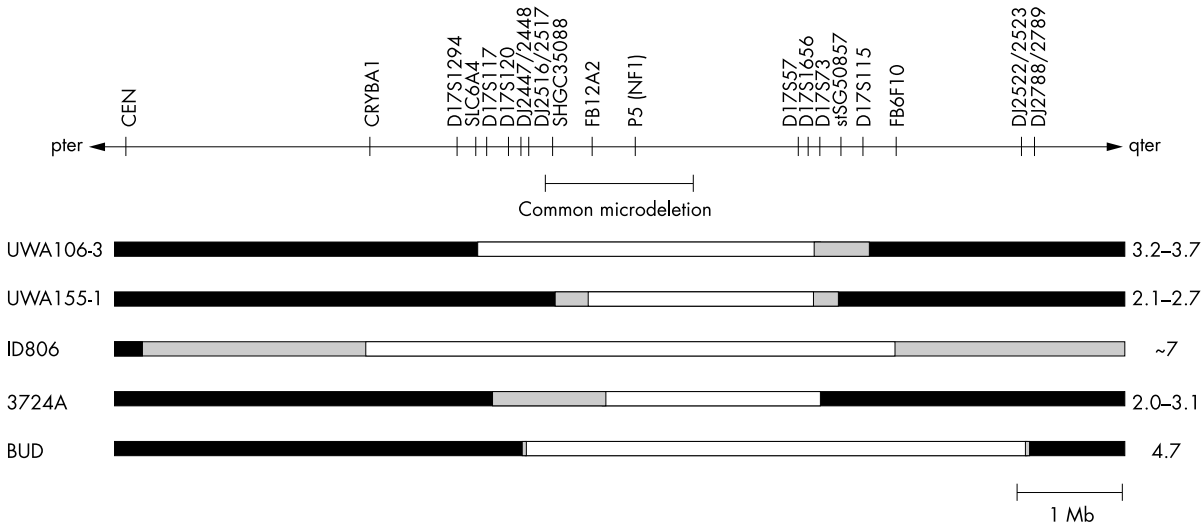

Figure 5 Comparison of large deletions between BUD and four other NF1 patients—UWA106-3,[9 15 16 19] UWA155-1,[9] ID806,[17] and 3724A.[5] Relevant plasmid probes (D17S120, D17S57, D17S73, D17S115) previously used to detect polymorphic fragments by Southern hybridisation analysis were sequenced and positioned within our clone contig (D17557 (AJ550808); D17573 (AJ550810); D175115 (AJ550811)). P5 indicates the location of an NF1 cDNA probe, which extends from exon 37 to the end of the coding sequence.[20] Black bars represent undeleted segments; deleted regions are marked as white bars; possibly deleted uncharacterised regions are given as grey bars. On the right, the respective deletion size is given in Mb.

breakpoints fall far beyond these boundaries and have not so far been located at the molecular sequence level.

The deletion of the patient BUD described here is more far reaching in telomeric direction and thus we extended our clone and sequence map up to the distal breakpoint. Major portions of this region have been sequenced and assembled as HTGS data by the Human Genome Consortium towards the end our studies and were partially reported recently.[21] The existence of low copy repeats on BAC 640N20 has prevented an automatic assembly of the adjoining telomeric region. Furthermore, some of the genes between the LCR on BAC R-640N20 and the distal breakpoint of patient BUD were not fully annotated and reviewed. We confirmed and fully established the map by FISH experiments with additional BAC and PAC clones that were initially screened to cover the deleted region fully.

Comparative analyses of the human and murine genome sequences enabled us to identify all functional genes that are co-deleted in our patient BUD and may contribute to the clinical phenotype (table 2; fig 3). Thus our patient is not only hemizygous for the 14 genes between the proximal and distal LCRs at 17q11.2, inclusive of the *NF1* gene, but also for the 27 genes following distally.

The most conspicuous clinical finding in patient BUD is the large number of bilateral spinal neurofibromas. Although spinal neurofibromas develop as isolated asymptomatic tumours in up to 36% of NF1 patients,[22–24] multiple symmetrically distributed spinal tumours with clinical implications are very rare in classical NF1 patients. Familial spinal neurofibromatosis (FSNF, MIM 162210) is a rare distinct form of NF1 which is characterised by multiple symmetrical spinal nerve root neurofibromas and café au lait spots in all affected family members.[25] FSNF is associated with NF1 mutations, but is not caused by specific mutations in the NF1 gene.[26–28] It has been suggested that a gene closely linked to the *NF1* locus is modifying the NF1 phenotype in FSNF.[28] Most probably, the analyses of large deletion patients with or without multiple spinal neurofibromas will help to identify this modifying locus. Unfortunately, a search for spinal neurofibromas by MRI has not been done in the patients ID806 and 3724A. Patient UWA155-1 was reported to have one spinal neurofibroma, but it is unknown whether he carries multiple asymptomatic spinal tumours.[9] However, patient BUD, described here, and patient UWA106-3,[9] who both have large deletions, developed numerous spinal tumours.

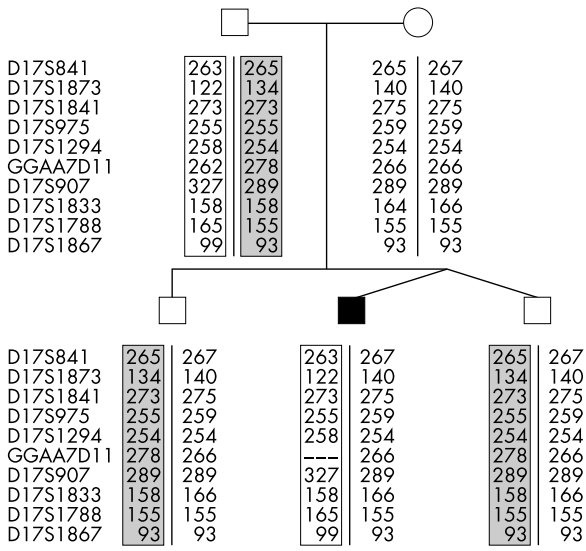

Figure 6 Haplotype reconstruction of 10 polymorphic markers at 17q11.2-12 in the family of patient BUD. Markers D17S841, D17S1873, D17S1841, D17S975, and D17S1294 are proximal to the deleted interval, whereas marker GGAA7D11is located in the deleted region. Markers D17S907, D17S1833, D17S1788, and D17S1867 are distal to the telomeric deletion breakpoint. As indicated by an unfilled rectangle, the deletion occurred on the paternal haplotype by an intrachromosomal mechanism.

As the number of spinal neurofibromas has not been investigated and quantitated systematically by MRI in patients with LCR mediated NF1 microdeletion, we cannot really exclude the genes of the 1.4 mbp interval, but in view of the clinical data reported so far, we suggest that one of the genes distal to the 1.4 mbp interval is implicated in the development of spinal neurofibromas. The most suspicious region for such a locus is the segment between the distal NF1 LCR and the marker FB6F10, which is deleted in both patients and encompasses nine functional genes. Hemizygosity with reduced activity of this modifier gene might predispose patients BUD and UWA106-3 to the development of multiple spinal neurofibromas. Similarly, a mutation in the modifier locus or a hypomorphic allele of the latter could contribute to the phenotype in patients with FSNF.

Comparing the breakpoint regions in patient BUD at the sequence levels, we did not encounter blocks of low copy repeats around the proximal and distal breakpoints, which could have triggered chromosomal mispairing and unequal homologous recombination during meiosis, as has been observed in patients with 1.4 mbp deletions.[11 13] The proximal breakpoint of BUD is located between position 49221 and 81044 on BAC R-271K11 (AC005562), about 65 kbp centromeric to the proximal *LCR* of the *NF1* gene region, which triggers the common 1.4 mbp deletion by recombination with the distal LCR.

A third LCR, which is similar to the regional LCRs at 17q11.2, has been mapped to 17q24.[9] This distal LCR also contains fragments of the *WI-12393* gene. Our mapping of the deletion breakpoint in patient BUD rules out the involvement of another *WI-12393* derived LCR, including the one at 17q24.

The comparisons of the long range deletions at 17q in five different patients including our patient BUD[5 9 10 15–17] strongly suggest that all deletion breakpoints in these patients are unique and do not coincide with pairs of LCRs situated at the proximal and distal boundaries.

The fact that the distal breakpoints in three patients (UWA106-3, 155-1, and patient 3724A[5 9 15]) occur within the 1 mbp spanning the *ACCN1* gene suggests that this region is accessible and transcribed during germ cell development. The distal deletion breakpoint of patient BUD, however, maps far away from the *ACCN1* gene to the region of the *SLFN* genes. In the region around the distal deletion boundary of patient BUD, the human and the mouse genomes again displayed significant discrepancies. Comparing the *SLFN* genes, we noticed only six human members *(SLFN1-6)* of the *SLFN* gene family in the human genome, but 10 murine genes in the otherwise conserved human–mouse interval (fig 4). These findings indicate that the *SLFN* gene region has been reshaped by multiple breaks and subsequent rearrangements during the evolution of rodents and humans, and that the deletion of patient BUD occurred in this region of recent evolutionary rearrangements.

The proximal deletion breakpoint of patient BUD falls within a 200 kbp large gene-free segment represented by BAC R-271K11. This BAC spans various blocks of low copy repeats—a partial SMS-REP,[29] a *SMURF2* pseudogene fragment, the known *WI-12393* related LCR, sequences from chromosome 19—and is followed by the *KIAA0160* pseudogene

fragment covered by the BAC R-778K9. These blocks originate from different genomic locations and have been inserted successively into this region during primate evolution.[14] We therefore suggest that the proximal breakpoint region again carries intrinsic features which facilitate double stranded breaks and rearrangements.

Approximately 80% of small intragenic mutations are paternally inherited,[30–32] whereas meiotically generated microdeletions of the *NF1* gene region are predominantly of maternal origin.[6 8 9 32 33] In 17 of 19 informative cases (89%) analysed by López-Correa *et al*,[13] the deletions occurred on the maternal allele. By contrast, the deletions of patient UWA106-3,[15 16] patient ID806,[17] patient 96-2,[12 33] and patient PF[12] that do not end at the proximal and distal NF1 LCRs were of paternal origin, with one exception (patient 3724A[5]).

To gain insight into the mechanism of recombination, six families containing patients with de novo deletions were previously analysed by haplotyping.[33] All five deletions on the maternal chromosome occurred by crossovers between non-sister chromatids, whereas the paternal chromosome acquired a de novo deletion by intrachromosomal (sister chromatid) breaks. Interestingly, this latter deletion (patient 96-2) is not bordered by LCRs and is probably restricted to the *NF1* gene. Likewise, the deletion of patient BUD arose by an intrachromosomal mechanism during male germ cell development. Length variation of deletions across the NF1 locus were also observed in neurofibromas of NF1 patients which lost the normal NF1 allele by a mitotically acquired interstitial deletion of the normal 17-homologue.[34] As shown previously, even interstitial deletions between LCRs can occur intrachromosomally during mitosis in somatic cells, probably driven by the recombination between misaligned LCRs in sister chromatids.[35 36] In view of these observations it seems quite reasonable to assume that non-LCR-driven interstitial deletions are primarily generated during mitotic cell division in particular in the course of spermatogenesis.

ACKNOWLEDGEMENTS

We thank Wolfgang Lasinger, Helene Spöri, Karin Lehmann, and Antje Kollak for expert technical assistance, and Dr Upadhyaya for sending us various 17q-marker plasmids. This research was supported by grants from the Deutsche Forschungsgemeinschaft (HA1082 and KE-724 2-1 (to HK-S) and KFO 113-1 (To DEJ)) and the Deutsche Krebshilfe (No 70-2452/project 790-3075-Ti).

Authors' affiliations

H Kehrer-Sawatzki, Department of Human Genetics, University of Ulm, Ulm, Germany
S Tinschert, Institute of Medical Genetics, Charité, Humboldt-University, Berlin, Germany
D E Jenne, Department of Neuroimmunology, Max-Planck-Institute of Neurobiology, Martinsried, Germany

Correspondence to: Dr Dieter E. Jenne, Department of Neuroimmunology, Max-Planck-Institute of Neurobiology, Am Klopferspitz 18a, Planegg-Martinsried D-82152, Germany; djenne@neuro.mpg.de

REFERENCES

1 **Friedman JM**, Gutmann DH, MacCollin M, *et al*. Phenotype, natural history and pathogenesis. In: *Neurofibromatosis*. Baltimore: John Hopkins University Press, 1999.
2 **Huson SM**, Hughes RAC. A pathogenetic and clinical overview. In: *The Neurofibromatoses*. London: Chapman and Hall, 1994.
3 **Heim RA**, Kam-Morgan LN, Binnie CG, *et al*. Distribution of 13 truncating mutations in the neurofibromatosis 1 gene. *Hum Mol Genet* 1995;**4**:975–81.
4 **Fahsold R**, Hoffmeyer S, Mischung C, *et al*. Minor lesion mutational spectrum of the entire *NF1* gene does not explain its high mutability but points to a functional domain upstream of the GAP-related domain. *Am J Hum Genet* 2000;**66**:790–818.
5 **Cnossen MH**, van der Est MN, Breuning MH, *et al*. Deletions spanning the neurofibromatosis type 1 gene: implications for genotype-phenotype correlations in neurofibromatosis type 1? *Hum Mutat* 1997;**9**:458–64.
6 **Valero MC**, Pascual-Castroviejo I, Velasco E, *et al*. Identification of de novo deletions at the *NF1* gene: no preferential paternal origin and phenotypic analysis of patients. *Hum Genet* 1997;**99**:720–6.
7 **Rasmussen SA**, Colman SD, Ho VT, *et al*. Constitutional and mosaic large *NF1* gene deletions in neurofibromatosis type 1. *J Med Genet* 1998;**35**:468–71.
8 **Upadhyaya M**, Ruggieri M, Maynard J, *et al*. Gross deletions of the neurofibromatosis type 1 (*NF1*) gene are predominantly of maternal origin and commonly associated with a learning disability, dysmorphic features and developmental delay. *Hum Genet* 1998;**102**:591–7.
9 **Dorschner MO**, Sybert VP, Weaver M, *et al*. NF1 microdeletion breakpoints are clustered at flanking repetitive sequences. *Hum Mol Genet* 2000;**9**:35–46.
10 **Jenne DE**, Tinschert S, Stegmann E, *et al*. A common set of at least 11 functional genes is lost in the majority of NF1 patients with gross deletions. *Genomics* 2000;**66**:93–7.
11 **Jenne DE**, Tinschert S, Reimann H, *et al*. Molecular characterization and gene content of breakpoint boundaries in patients with neurofibromatosis type 1 with 17q11.2 microdeletions. *Am J Hum Genet* 2001;**69**:516–27.
12 **López-Correa C**, Brems H, Lazaro C, *et al*. Molecular studies in 20 submicroscopic neurofibromatosis type 1 gene deletions. *Hum Mutat* 1999;**14**:387–93.
13 **López-Correa C**, Dorschner M, Brems H, *et al*. Recombination hotspot in *NF1* microdeletion patients. *Hum Mol Genet* 2001;**10**:1387–92.
14 **Jenne DE**, Tinschert S, Dorschner MO, *et al*. Complete physical map and gene content of the human *NF1* tumor suppressor region in man and mouse. *Genes Chrom Cancer* 2003;**37**:111–20.
15 **Kayes LM**, Riccardi VM, Burke W, *et al*. Large de novo DNA deletion in a patient with sporadic neurofibromatosis 1, mental retardation and dysmorphism. *J Med Genet* 1992;**29**:686–90.
16 **Kayes LM**, Burke W, Riccardi VM, *et al*. Deletions spanning the neurofibromatosis I gene: identification and phenotype of five patients. *Am J Hum Genet* 1994;**54**:424–36.
17 **Upadhyaya M**, Roberts SH, Maynard J, *et al*. A cytogenetic deletion, del(17)(q11.22q21.1), in a patient with sporadic neurofibromatosis type 1 (NF1) associated with dysmorphism and developmental delay. *J Med Genet* 1996;**33**:148–52.
18 **Moreira ES**, Wiltshire TJ, Faulkner G, *et al*. Limb-girdle muscular dystrophy type 2G is caused by mutations in the gene encoding the sarcomeric protein telethonin. *Nat Genet* 2000;**24**:163–6.
19 **Shen S**, Battersby S, Weaver M, *et al*. Refined mapping of the human serotonin transporter (SLC6A4) gene within 17q11 adjacent to the CPD and *NF1* genes. *Eur J Hum Genet* 2000;**8**:75–8.
20 **Wallace MR**, Marchuk DA, Andersen LB, *et al*. Type 1 neurofibromatosis gene: identification of a large transcript disrupted in three NF1 patients. *Science* 1990;**249**:181–6.
21 **Van Roy N**, Vandesompele J, Berx G, *et al*. Localization of the 17q breakpoint of a constitutional 1;17 translocation in a patient with neuroblastoma within a 25-kb segment located between the ACCN1 and TLK2 genes and near the distal breakpoints of two microdeletions in neurofibromatosis type 1 patients. *Genes Chromosomes Cancer* 2002;**35**:113–20.
22 **Thakkar SD**, Feigen U, Mautner VF. Spinal tumours in neurofibromatosis type 1: an MRI study of frequency, multiplicity and variety. *Neuroradiology* 1999;**41**:625–9.
23 **Poyhonen M**, Leisti EL, Kytola S, *et al*. Hereditary spinal neurofibromatosis: a rare form of NF1? *J Med Genet* 1997;**34**:184–7.
24 **Egelhoff JC**, Bates DJ, Ross JS, *et al*. Spinal MR findings in neurofibromatosis types 1 and 2. *Am J Neuroradiol* 1992;**13**:1071–7.
25 **Carey JC**, Viskochil DH. Neurofibromatosis type 1: A model condition for the study of the molecular basis of variable expressivity in human disorders. *Am J Med Genet* 1999;**89**:7–13.
26 **Ars E**, Kruyer H, Gaona A, *et al*. A clinical variant of neurofibromatosis type 1: familial spinal neurofibromatosis with a frameshift mutation in the NF1 gene. *Am J Hum Genet* 1998;**62**:834–41.
27 **Kaufmann D**, Muller R, Bartelt B, *et al*. Spinal neurofibromatosis without cafe-au-lait macules in two families with null mutations of the NF1 gene. *Am J Hum Genet* 2000;**69**:1395–400.
28 **Messiaen L**, Riccardi V, Peltonen J, *et al*. Independent NF1 mutations in two large families with spinal neurofibromatosis. *J Med Genet* 2003;**40**:122–6.
29 **Park SS**, Stankiewicz P, Bi W, *et al*. Structure and evolution of the Smith-Magenis syndrome repeat gene clusters, SMS-REPs. *Genome Res* 2002;**12**:729–38.
30 **Jadayel D**, Fain P, Upadhyaya M, *et al*. Paternal origin of new mutations in von Recklinghausen neurofibromatosis. *Nature* 1990;**343**:558–9.
31 **Stephens K**, Kayes L, Riccardi VM, *et al*. Preferential mutation of the neurofibromatosis type 1 gene in paternally derived chromosomes. *Hum Genet* 1992;**88**:279–82.
32 **Lazaro C**, Gaona A, Ainsworth P, *et al*. Sex differences in mutational rate and mutational mechanism in the *NF1* gene in neurofibromatosis type 1 patients. *Hum Genet* 1996;**98**:696–9.
33 **López-Correa C**, Brems H, Lazaro C, *et al*. Unequal meiotic crossover: a frequent cause of *NF1* microdeletions. *Am J Hum Genet* 2000;**66**:1969–74.
34 **Colman SD**, Williams CA, Wallace MR. Benign neurofibromas in type 1 neurofibromatosis (NF1) show somatic deletions of the *NF1* gene. *Nat Genet* 1995;**11**:90–2.
35 **Petek E**, Jenne DE, Smolle J, *et al*. Mitotic recombination mediated by the *JJAZF1 (KIAA0160)* gene causing somatic mosaicism and a new type of constitutional *NF1* microdeletion in two children of a mosaic female with only few manifestations. *J Med Genet* 2003;**40**:520–5.
36 **Serra E**, Rosenbaum T, Nadal M, *et al*. Mitotic recombination affects homozygosity for NF1 germline mutations in neurofibromas. *Nat Genet* 2001;**28**:294–6.